

Tracking Surface Cyclones with Moist Potential Vorticity

Zuohao CAO*¹ and Da-Lin ZHANG²

¹*Meteorological Service of Canada, Ontario, Canada*

²*Department of Meteorology, University of Maryland, College Park, Maryland*

(Received 17 February 2004; revised 10 May 2004)

ABSTRACT

Surface cyclone tracks are investigated in the context of moist potential vorticity (MPV). A prognostic equation of surface absolute vorticity is derived which provides a basis for using negative MPV (NMPV) in the troposphere as an alternative approach to track surface cyclones. An observed case study of explosive lee cyclogenesis is performed to test the effectiveness of the MPV approach. It is shown that when a surface cyclone signal is absent due to the blocking of the Rocky Mountains, the surface cyclone can be well identified by tracing the peak NMPV.

Key words: cyclone track, moist potential vorticity, lee cyclogenesis

1. Introduction

There have been two different approaches used for tracking extratropical cyclones. The traditional and most common approach is to follow the minimum surface pressure of a cyclone (e.g., Petterssen, 1956; Carnell and Senior, 1998; Serreze, 1995; Blender et al., 1997), whereas the second approach is to find the regions of the maximized root-mean-square bandpass-filtered (2.5–6 days) geopotential height (e.g., Blackmon et al., 1977; Lau, 1988). In some cases, the second approach cannot uniquely identify true synoptic systems (e.g., Wallace et al., 1988; Carnell and Senior, 1998) and the resulting cyclone tracks are not quite the same as those defined traditionally. As a result, the cyclone tracks defined by the traditional approach are more objective than those defined by the second approach. Nevertheless, the traditional approach may not be effective in cases where surface cyclone signals are obscure or absent, e.g., due to the blocking of mountains, while the internal dynamics may indicate an ongoing process of intensive development. One may then wonder how to trace this type of atmospheric disturbance in the absence of surface cyclone signals.

Therefore, the objective of this study is to develop an alternative method to estimate the tracks of surface cyclones using upper-air meteorological information from the moist potential vorticity (MPV) perspec-

tive. The MPV is defined as

$$M_{\text{PV}} = \frac{1}{\rho} \zeta_{\text{a}} \cdot \nabla \theta_e, \quad (1)$$

where ζ_{a} , θ_e , and ρ are the absolute vorticity vector, equivalent potential temperature, and density, respectively. The MPV is chosen to track cyclone movements due to its simple expression and its enriched three-dimensional atmospheric information including dynamic, thermodynamic, and moisture processes. Since surface cyclones may be described in terms of surface absolute vorticity, their tracks can be elucidated in the context of MPV if the rate of change of surface absolute vorticity can be formulated as a function of MPV. This will be demonstrated in the next section.

Few studies in the past have been performed to explore the use of MPV for diagnosing extratropical cyclones, particularly for the surface cyclone tracking problem. Because MPV includes the moisture variable, it is different from potential vorticity (PV) (Hoskins et al., 1985; Davis and Emanuel, 1991; Huo et al., 1998) in terms of conservation and generation properties. MPV is conserved in a saturated atmosphere, and generated in unsaturated regions of three-dimensional flows. In other words, MPV is conserved in the presence of condensational heating, but PV is not. As found by Cao and Cho (1995) (hereafter referred to as CC), negative (positive) MPV can be generated in regions where baroclinic vectors have a component along (against) the direction of moisture gra-

*E-mail: zuohao.cao@ec.gc.ca

dients. Both observational and modeling studies have shown that $MPV < 0$ can be more readily satisfied in the extratropical cyclone/frontal systems (Thorpe and Clough, 1991; Cao and Moore, 1998) and mesoscale convective systems (Zhang and Cho, 1992; Wu and Liu, 1997) than $PV < 0$. We will show in this study that negative MPV (NMPV) can provide an effective way to trace surface cyclones.

The next section presents a theoretical basis for using MPV to trace surface cyclones. To show the effectiveness of the MPV approach, section 3 presents the applicability of the theory to an observed case in which a surface cyclone moved across the Western Cordillera when its surface signal was absent due to the topographic blocking. A summary and conclusions are given in the final section.

2. Theory

Based on the primitive equation system, the prognostic equations for MPV and absolute vorticity can be written as:

$$\begin{aligned} \frac{dM_{PV}}{dt} = & \left(\frac{\zeta_a}{\rho} \cdot \nabla \right) \frac{d\theta_e}{dt} + \nabla\theta_e \cdot \frac{\nabla\rho \times \nabla p}{\rho^3} \\ & + \nabla\theta_e \cdot \left(\frac{1}{\rho} \nabla \times \frac{\mathbf{F}}{\rho} \right), \end{aligned} \quad (2)$$

and

$$\begin{aligned} \frac{d\zeta_a}{dt} = & (\zeta_a \cdot \nabla)\mathbf{v} - \zeta_a \nabla \cdot \mathbf{v} + \frac{\nabla\rho \times \nabla p}{\rho^2} \\ & + \nabla \times \frac{\mathbf{F}}{\rho}, \end{aligned} \quad (3)$$

where p , \mathbf{F} , and \mathbf{v} are pressure, friction, and velocity, respectively.

The rate of change of surface absolute vorticity can then be formulated as a function of MPV from Eqs. (2) and (3). To demonstrate this, we substitute Eq. (3) into Eq. (2) making use of vector identities, integrate the resulting equation over the volume V making use of the Gaussian theorem, and finally yield an equation for the rate of change of absolute vorticity on any arbitrary low-level surface S_L (Fig. 1):

$$\begin{aligned} \int_{S_L} \frac{\theta_e}{\rho} \frac{d\zeta_a}{dt} \cdot ds = & - \int_{S-S_L} \frac{\theta_e}{\rho} \frac{d\zeta_a}{dt} \cdot ds + \oint_S \frac{\theta_e}{\rho} [(\zeta_a \cdot \nabla)\mathbf{v} \\ & - \zeta_a \nabla \cdot \mathbf{v} + \nabla \times \frac{\mathbf{F}}{\rho}] \cdot ds \\ & + \int_V \left[\frac{dM_{PV}}{dt} - \left(\frac{\zeta_a}{\rho} \cdot \nabla \right) \frac{d\theta_e}{dt} \right. \\ & \left. - \nabla\theta_e \cdot \left(\frac{1}{\rho} \nabla \times \frac{\mathbf{F}}{\rho} \right) \right] dv, \end{aligned} \quad (4)$$

where S denotes a surface surrounding the volume V . Without loss of generality, the integration of Eq. (4) can be performed in any atmospheric column with any size of surface S . As shown in Fig. 1, the direction of the surface S_L normal is opposite to that of the surface absolute vorticity ζ_a . Therefore, Eq. (4) can be written in another form:

$$\begin{aligned} \int_{S_L} \frac{\theta_e}{\rho} \frac{d\zeta_a}{dt} \cdot ds = & \int_{S-S_L} \frac{\theta_e}{\rho} \frac{d\zeta_a}{dt} \cdot ds - \oint_S \frac{\theta_e}{\rho} [(\zeta_a \cdot \nabla)\mathbf{v} \\ & - \zeta_a \nabla \cdot \mathbf{v} + \nabla \times \frac{\mathbf{F}}{\rho}] \cdot ds - \int_V \left[\frac{dM_{PV}}{dt} \right. \\ & \left. - \left(\frac{\zeta_a}{\rho} \cdot \nabla \right) \frac{d\theta_e}{dt} - \nabla\theta_e \cdot \left(\frac{1}{\rho} \nabla \times \frac{\mathbf{F}}{\rho} \right) \right] dv, \end{aligned} \quad (5)$$

where $\int_V (dM_{PV}/dt)dv$ is the rate of change of MPV, or the generation of MPV, in the volume V .

Equation (5) relates the rate of change of lower-level absolute vorticity to the rate of change of upper-level and lateral absolute vorticity, the tilting of absolute vorticity, the divergence, and friction over the surface S , as well as the MPV generation in the atmospheric column. In the PV framework, however, no such a relationship can be derived between the lower-level absolute vorticity and the PV generation.

The importance of MPV generation, $\int_V (dM_{PV}/dt)dv$, with respect to the rate of change of lower-level absolute vorticity, $\int_{S_L} (\theta_e/\rho)(d\zeta_a/dt)ds$, can be demonstrated using a scale analysis. These two terms

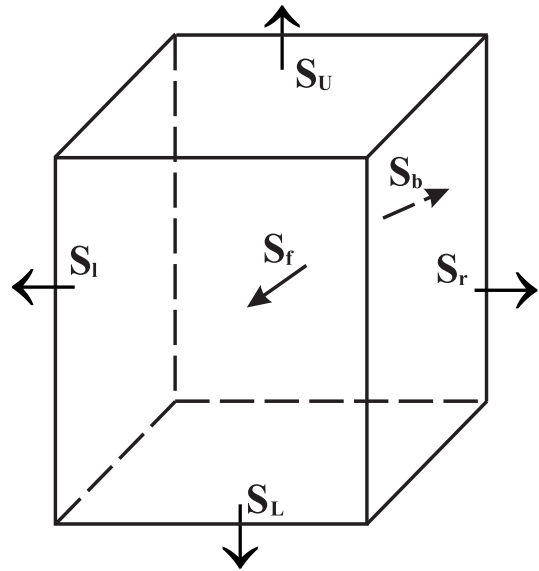


Fig. 1. A schematic diagram showing an integration over the volume V enclosed by the surface S , where $S = S_U + S_L + S_L + S_f + S_r + S_b$. The vectors indicate the normals perpendicular to the corresponding surfaces.

can be approximately expressed as an average over the surface S_L and the volume $V(= S_L H)$:

$$\frac{\theta_e}{\rho} \frac{d\zeta_a}{dt} S_L \propto -\frac{1}{\rho} \zeta_a \cdot \frac{d\nabla\theta_e}{dt} S_L H, \quad (6)$$

where H is a depth scale. The term $(\zeta_a/\rho) \cdot (d\nabla\theta_e/dt)$ is a part of $d[(\zeta_a/\rho) \cdot \nabla\theta_e]/dt$, and it is highly dependent on the frontogenetical function $d\nabla\theta_e/dt$. Based on Bond and Fleagle (1985), the magnitude of the frontogenetical function varies from 10^{-10} to 10^{-4} K m⁻¹ s⁻¹, which is resolution- and case-dependent. If we use a typical atmospheric value of 10^{-8} K m⁻¹ s⁻¹, together with $\zeta_a=10^{-4}$ s⁻¹, $d\zeta_a/dt=10^{-10}$ s⁻², $\theta_e=300$ K, $\rho=1$ kg m⁻³, and $H=10^4$ m, it is easy to show that the two terms have the same order of magnitude of 10^{-8} K m³ kg⁻¹ s⁻².

3. Application to an observed event

As mentioned in the introduction, in forecast practice, the surface cyclone signals may be absent due to various reasons. A good example is the filling of a cyclone on the windward side as it moves across a major mountain range. However, this type of cyclone may slowly intensify due to its internal dynamics or latent heat release associated with uplifting. Since MPV includes these upper-level dynamic and thermodynamic processes, it is possible to track this type of surface cyclone using the approach described in section 2.

For this purpose, an explosive cyclogenesis event that occurred during 1–3 April 1982 is selected. The associated MPV field is calculated using the National Center for Environmental Prediction (NCEP) reanalysis archived at the Canadian Meteorological Centre (CMC). The analysis fields include geopotential height, temperature, dew-point depression, and horizontal winds, which are extracted from the archive with a horizontal resolution of $2.5^\circ \times 2.5^\circ$ and 17 constant pressure levels at 1000, 925, 850, 700, 600, 500, 400, 300, 250, 200, 150, 100, 70, 50, 30, 20, and 10 hPa. The NCEP reanalysis data used in this study have a time interval of 6 hours. These fields are then interpolated onto a grid mesh with a resolution of $1.0^\circ \times 1.0^\circ$. After computing the three-dimensional MPV field from the analysis data, we then search for the peak NMPV in the vertical and plot the NMPV at that level. Finally, the center of the peak NMPV on that level is positioned, and considered as the cyclone center.

Since the mean sea level pressure field is not available in the CMC archive of the NCEP reanalysis, geopotential heights on the 1000-hPa pressure sur-

face are presented in Fig. 2. This cyclone experienced three major phases with different characteristics in each stage. During the first phase from 0000 UTC to 1200 UTC 1 April, the parent cyclone from the Pacific Ocean filled as it moved along the upslope of the Rocky Mountains (Figs. 2a, b). Meanwhile, the cyclone was being split into two parts (Fig. 2b). The point of interest is that on the downslope side of the Rocky Mountains, the cyclone did not show any signal of genesis (Figs. 2b, c). This is consistent with many of the previous climatological studies in which extratropical cyclones rarely maintained their identities in the surface analyses as they moved across the Rockies (e.g., Gyakum et al., 1996). The second phase started from 1200 UTC 1 April to 1200 UTC 2 April (not shown) and was detailed by Hu and Reiter (1987) using the conventional sounding data. They noted that the cyclone experienced an explosive deepening between 0000 and 1200 UTC 2 April when it moved to the east of the Rocky Mountains. The third phase extended from 1800 UTC 2 to 1800 UTC 3 April. During this period, this cyclone moved eastward and then became quasi-stationary over the Province of Ontario, Canada. A maximum surface wind of 38 m s⁻¹ was observed near Lake Superior. Heavy rainfall caused flooding conditions along the northern shores of Lake Erie with reported 2-m waves. Heavy snow and blowing snow, combining with temperatures below -15°C , resulted in severe conditions over Ontario (Lewis, 1987). From 1200 UTC 1 April to 1800 UTC 3 April, this cyclone traveled about 3300 km from the lee of the Rocky Mountains to the Great Lakes region.

While the surface analysis does not show any signal of cyclogenesis on the lee of the Rocky Mountains (Figs. 2b, c), its associated MPV field does show a strong signal of the development of a cyclonic circulation (Figs. 3a, b). Specifically, the peak NMPV on the 300-hPa pressure surface was centered near (50°N , 110°W), which was almost at the same position as the cyclone center at 1200 UTC 1 April (cf. Figs. 3a and 3b). This shows that although anticyclonic tendencies may occur as the surface cyclone moves over the upslope (Mass and Dempsey, 1985), its associated upper-level forcings favorable for cyclogenesis can still be detected in terms of MPV. In this regard, the MPV approach can fill the gap of the traditional method in tracking surface cyclones when they travel across high mountains and lose identities (Gyakum et al., 1996). It is evident from 0000 to 1200 UTC 1 April that the upper-level NMPV was persistent over the regions where the surface cyclone “developed” (Figs. 3a and 3b). After the cyclone pass-

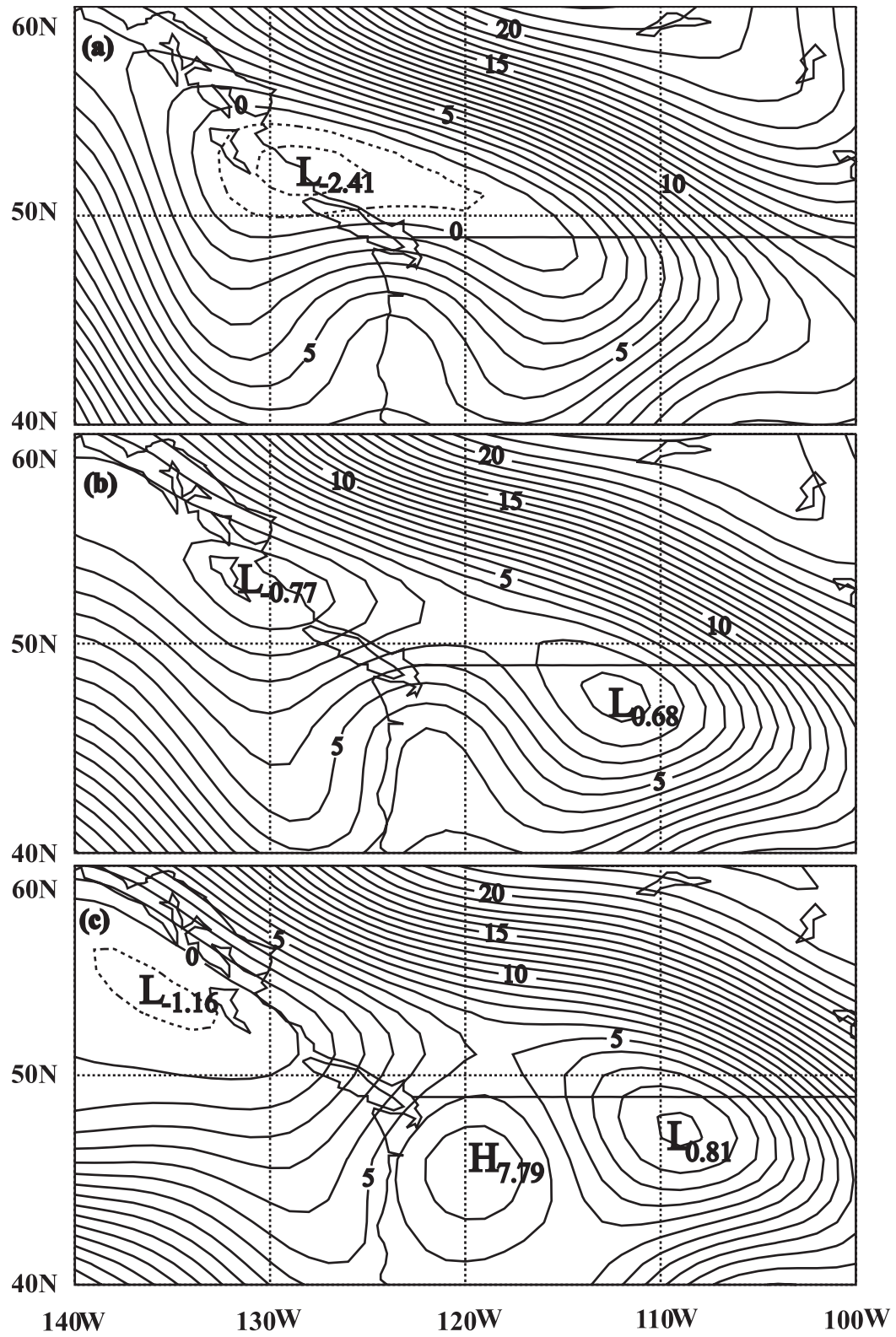


Fig. 2. Distribution of 1000-hPa geopotential height at intervals of 1 dam at (a) 0000, (b) 0600, and (c) 1200 UTC 1 April 1982.

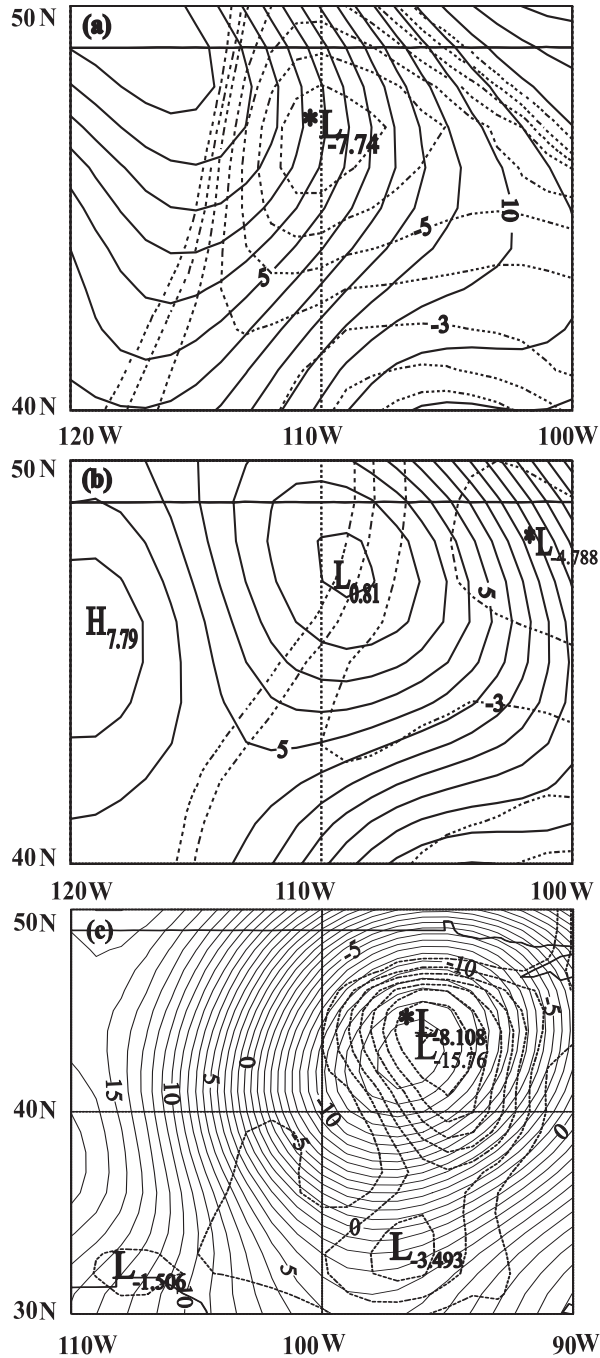


Fig. 3. Distribution of 1000-hPa geopotential height (solid lines) at intervals of 1 dam, and NMPV (dashed lines) in units of 0.1 PVU ($1 \text{ PVU} = 10^{-6} \text{ K m}^{-2} \text{ s}^{-1} \text{ kg}^{-1}$) at (a) 0000 UTC 1 April 1982 on the 300-hPa pressure surface, (b) 1200 UTC 1 April 1982 on the 300-hPa pressure surface, and (c) 1800 UTC 2 April 1982 on the 850-hPa pressure surface. Symbol * indicates the location of the peak NMPV.

ed over the Rocky Mountains, the peak NMPV was well co-located with the low pressure center, indicating

the presence of possible phase locking between the surface cyclone and the peak NMPV (Fig. 3c). It should be pointed out that when the cyclone was traveling, the peak NMPV was positioned ahead of the surface low pressure center (Figs. 3a, b). After the cyclone became stationary, the peak NMPV was found at the low pressure center. This may be a result of the spatial and temporal dependence of the maximum frontogenetical function [(see Eq. (6)).

4. Summary and conclusions

In this study, an alternative approach for tracking surface cyclones is developed in terms of MPV. A prognostic equation for surface absolute vorticity is derived which relates the NMPV generation to the surface cyclone movements.

The MPV approach is then applied to an observed cyclone. It is shown that although the signals of surface cyclogenesis are absent due to the blocking of the Rocky Mountains, the cyclone track can be well identified as it moves across the major mountain range. In this regard, the present MPV approach can fill a gap in the traditional approach for tracking surface cyclones.

In conclusion, we may state that the MPV approach developed in this study can be an alternative way to consistently track surface cyclones using the upper-level meteorological information. In general, the traditional approach can better resolve the cyclone tracks due to more available observations at the surface than those at the upper levels. However, when the surface cyclone signals are obscure, the MPV approach can provide useful guidance for tracking cyclone movements because of the more three-dimensional dynamics and thermodynamics involved in the MPV parameter. In a forthcoming article, more case studies will be conducted to compare the performance of the current MPV approach to those used in previous studies.

REFERENCES

- Blackmon, M. L., J. M. Wallace, N.-C. Lau, and S. L. Mullen, 1977: An observational study of the Northern Hemisphere wintertime circulation. *J. Atmos. Sci.*, **34**, 1040–1053.
- Blender, R., K. Fraedrich, and F. Lunkeit, 1997: Identification of cyclone-track regimes in the North Atlantic. *Quart. J. Roy. Meteor. Soc.*, **123**, 727–741.
- Bond, N. A., and R. G. Fleagle, 1985: Structure of a cold front over the ocean. *Quart. J. Roy. Meteor. Soc.*, **111**, 739–759.
- Cao, Z., and H.-R. Cho, 1995: Generation of moist potential vorticity in extratropical cyclones. *J. Atmos. Sci.*, **52**, 3263–3281.
- Cao, Z., and G. W. K. Moore, 1998: A diagnostic study of moist potential vorticity generation in an extratropical cyclone. *Adv. Atmos. Sci.*, **15**, 152–166.

- Carnell, R. E., and C. A. Senior, 1998: Changes in mid-latitude variability due to increasing greenhouse gases and sulphate aerosols. *Climate Dyn.*, **14**, 369–383.
- Davis, C. A., and K. A. Emanuel, 1991: Potential vorticity diagnosis of cyclogenesis. *Mon. Wea. Rev.*, **119**, 1929–1953.
- Gyakum, J., D.-L. Zhang, J. Witte, K. Thomas, and W. Wintels, 1996: CASP II and Canadian cyclones during the 1989–92 cold seasons. *Atmos.-Ocean*, **34**, 1–16.
- Hoskins, B. J., M. E. McIntyre, and A. W. Robertson, 1985: On the use and significance of isentropic potential vorticity maps. *Quart. J. Roy. Meteor. Soc.*, **111**, 877–946.
- Hu, Q., and E. R. Reiter, 1987: A diagnostic study of explosive cyclogenesis in the lee of the Rocky mountains. *Meteor. Atmos. Phys.*, **36**, 161–184.
- Huo, Z., D.-L. Zhang, and J. Gyakum, 1998: An application of potential vorticity inversion to improving the numerical prediction of the March 1993 superstorm. *Mon. Wea. Rev.*, **126**, 424–436.
- Lau, N.-C., 1988: Variability of the observed midlatitude storm tracks in relation to low-frequency changes in the circulation pattern. *J. Atmos. Sci.*, **45**, 2718–2743.
- Lewis, P. J., 1987: Severe storms over the Great Lakes: A catalogue summary for the period 1957 to 1985. Canadian Climate Center Rep. 87-13, Meteorological Service of Canada, Downsview, ON, Canada, 342pp. [Available from Climatological Services Division, Meteorological Service of Canada, 4905 Dufferin St., Downsview, ON M3H 5T4, Canada.]
- Mass, C. F., and D. P. Dempsey, 1985: A one-level, mesoscale model for diagnosing surface winds in mountainous and coastal regions. *Mon. Wea. Rev.*, **113**, 1211–1227.
- Petterssen, S., 1956: *Weather Analysis and Forecasting*. Vol. 1, McGraw-Hill, 428pp.
- Serreze, M. C., 1995: Climatological aspects of cyclone development and decay in the Arctic. *Atmos.-Ocean*, **33**, 1–23.
- Thorpe, A. J., and S. A. Clough, 1991: Mesoscale dynamics of cold fronts: Structures described by dropsoundings in FRONTS 87. *Quart. J. Roy. Meteor. Soc.*, **117**, 903–941.
- Wallace, J. M., G.-H. Lim, and M. L. Blackmon, 1988: On the relationship between cyclone tracks, anticyclone tracks and baroclinic waveguides. *J. Atmos. Sci.*, **45**, 439–462.
- Wu, G., and H. Liu, 1997: Vertical vorticity development owing to down-sliding at slantwise isentropic surface. *Dyn. Atmos. Oceans*, **27**, 715–743.
- Zhang, D.-L., and H.-R. Cho, 1992: The development of negative moist potential vorticity in the stratiform region of a simulated squall line. *Mon. Wea. Rev.*, **120**, 1322–1341.